Earthquakes and Structures, *Vol. 14, No. 1 (2018) 33-44*
DOI: https://doi.org/10.12989/eas.2018.14.1.033

Effect of the incoherent earthquake motion on responses of seismically isolated nuclear power plant structure

Kaiser Ahmed[1a], Dookie Kim[*1] and Sang H. Lee[2b]

[1]*Department of Civil Engineering, Kunsan National University, Gunsan-si, 54150, Republic of Korea*
[2]*Power Engineering Research Institute, KEPCO E&C, Gimcheon, Republic of Korea*

(Received November 22, 2016, Revised January 15, 2018, Accepted January 20, 2018)

Abstract. Base-isolated nuclear power plant (BI-NPP) structures are founded on expanded basemat as a flexible floating nuclear island, are still lacking the recommendation of the consideration of incoherent motion effect. The effect of incoherent earthquake motion on the seismic response of BI-NPP structure has been investigated herein. The incoherency of the ground motions is applied by using an isotropic frequency-dependent spatial correlation function to perform the conditional simulation of the reference design spectrum compatible ground motion in time domain. Time history analysis of two structural models with 486 and 5 equivalent lead plug rubber bearing (LRB) base-isolators have been done under uniform excitation and multiple point excitation. two different cases have been considered: 1) Incoherent motion generated for soft soil and 2) Incoherent motion generated for hard rock soil. The results show that the incoherent motions reduce acceleration and the lateral displacement responses and the reduction is noticeable at soft soil site and higher frequencies.

Keywords: incoherent earthquake motion; base-isolated nuclear power plant; seismic response

1. Introduction

Differences in the amplitudes and phase angles of the seismic ground motions (GMs), recorded over extended areas has been recognized for many years. In the early days, lack of an adequately large set of recorded data prevented quantification of the phenomenon and the development of approaches for the incorporation of the effect into the dynamic analysis of nuclear safety related structures (forthcoming ASCE-4). Abrahamson (2007), in a separate study referenced herein, presents a state-of-the-art representation of the coherency function based on a large number of densely spaced ground motion recordings. Coherency functions define the relationships between ground motion at separate locations as a function of two parameters (1) the separation distance between the locations and (2) the frequency of the ground motion. For coherent motion and vertically propagating seismic waves, the amplitude at all locations is the same such that the coherency function is unity. For incoherent motion, the amplitude at separated distances is different and the coherency function is below unity (Abrahamson 2005, 2007). For fixed base NPP Horizontal and vertical ground motions are subject to incoherency and have been included (Abrahamson 2005, EPRI 2006).

∗Corresponding author, Professor
E-mail: kim2kie@kunsan.ac.kr
[a]Masters Graduate
E-mail: kaiser_ce_07@kunsan.ac.kr
[b]Senior Researcher
E-mail: shljrl@kepco-enc.com

Novak and Hindy (1979), Hindy and Novak (1980) were the pioneers to introduced the ground motion's coherency losses as a mathematical description in the earthquake engineering field. Early in the nineteen ninety eighties (Loh *et al*. 1982, Der Kiureghian *et al*. 1992, Abrahamson *et al*. 1991, 1993) addressed the phenomenon of incoherency based on the investigation on the earthquake acceleration recorded over limited regions. Later, comprehensive researches has been carried out by Luco *et al*. (1986) on rigid foundation, Hao *et al*. (1996) on asymmetric structures, Monti *et al*. (1996), Harichandran *et al*. (1996), Saxena *et al*. (2000), Kim *et al*. (2003), Chakraborty and Basu (2008), Mwafy *et al*. (2011) on nonlinear responses of long span bridges, highway bridges subjected to incoherent motions. Recently, Hossein *et al*. (2013) proposed method to generate spatially varying accelerograms using neural networks. According to Ghiocel *et al*. (2009) the effects of motion incoherency on the computed In-structure-response-spectra (ISRS) are significant for both the rock and the soil sites for NPP structures. Sayed *et al*. (2015) investigated spatial variation of El-Centro (1940) record for BI-NPP, Adanur *et al*. (2016), recommended to consider incoherent motion for suspension bridges isolated with LRBs.

Seismic (base) isolation is a mature technology in the civil engineering realm for protecting structures from the effects of moderate and severe earthquake shaking. Base-isolation being limitedly used in nuclear power plants, is a practical strategy that ensure the structural safety and flexibility in moderate to strong earthquake. Ali Hadidi *et al*. (2016) provided design of base-isolated buildings subjected to near fault motions, Mavronicola *et al*. (2014) investigated responses of bilinear LRB isolator under pulse-like motions. In addition, Murase *et al*. (2013) proposed a hybrid base-isolation system to improve seismic performances

http://www.techno-press.com/journals/eas&subpage=7 ISSN: 2092-7614 (Print), 2092-7622 (Online)

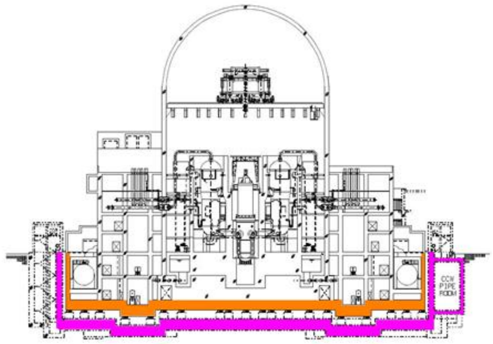

(a) Elevation

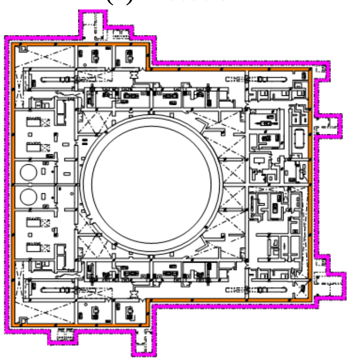

(b) Plan view

Fig. 1 Vertical and horizontal cross sections of the nuclear island

under pulse-like motions and long period motions. However, application of this technology still faces the shortcoming of adequate lack of design and construction guidelines. Seismic isolation has only been applied to six nuclear reactors in two nuclear power plants (NPPs), which are located in France and South Africa (Malushte and Whittaker 2005, Huang *et al*. 2007, 2010). Codes and standards for the analysis, design and construction of base-isolated nuclear power plants need to be established more vigorously through practical, deep and advanced researches. To date, according to forthcoming ASCE-4, the isolation system shall be analyzed and designed for three components of translational motion, two horizontal and one vertical, shall be input at the boundaries of the mathematical model only.

In this research, both, uniform and multi-support excitation of Kocaeli ground motions are applied to the BI-NPP to investigate the seismic responses. The computer program SIMQKE-II is used to perform the conditional simulation of Kocaeli earthquake ground motion in a hard rock site and soft rock site. Moreover, the influence of installing different numbers of the lead rubber bearing (LRB) isolators is investigated on the seismic responses of the BI-NPP. Two structural models of the BI-PP i.e., 486 isolators and 5 equivalent isolator models are analyzed under incoherent motion and compared with the seismic responses of uniform motion.

Unlike other conventional structures, BI-NPP structures are so heavy, founded on expanded base mate as a flexible floating nuclear island. As, seismic base-isolation of NPP is relatively challenging, extensive care must be taken to analyze and design while adopting this new technology. Nonetheless, very few studies have been conducted to study and examine the seismic responses of BI-NPPs considering spatially varying ground motions. Therefore, the issue of considering incoherent motion effect on BI-NPP is very important and needs to be resolved in the current seismic design code through comprehensive investigation. In this study, the incoherency of the ground motions is applied by using an isotropic frequency-dependent spatial correlation function to perform the conditional simulation of the reference design spectrum compatible ground motion in time domain. The lateral displacement, acceleration response spectra and ratio of uniform to incoherent motion responses are investigated and compared with uniform excitation.

2. Base-Isolated NPP structural model

2.1 Super structure

This numerical model is based on the APR1400, which stands for Advanced Power Reactor. The APR 1400 is a pressurized water reactor developed in Korea that produces 1400 MW of electrical power. Fig. 1(a) shows vertical and Fig. 1(b) shows horizontal cross sections of the nuclear island. APR 1400 featured Archetype Nuclear Test model (ANT) nuclear island, designed by KEPCO E&C, focuses on the behavior and analysis result of isolators. This is why, the same superstructure has been investigated for different numbers of isolator installed beneath the superstructure.

Main geometric dimension of the plan is: 103.6 m×102.4 m (340.0 ft.×336.0 ft.), pedestal dimensions (W×D×H): 2.44 m×2.44 m×1.80 m. The single numerical model of the superstructure of the APR 1400 nuclear island has been adopted where the total structure is analyzed with two different base-isolation configurations. To facilitate this effort, stick model of the Archetype Nuclear Test model (ANT) has been modelled incorporating 486 isolators and 5 equivalent isolator model in the OpenSees module.

Table 1 gives a summary on the size of superstructure where total number of nodes, beam elements, plate elements, mass elements and rigid body elements are illustrated. The beam elements are usually two-node connected elements allowing shear deformation whereas plate elements are thin shell elements without transverse shear deformation. The ANT numerical model includes the Nuclear Island (NI) buildings, the bearings supporting the nuclear island, bearing pedestals, and a lower basemat. The

Table 1 Size of the superstructure

Names	Size	Description
Nodes	1168	
Beam elements	71	Two-node, shear deformable beam
Plate elements	1033	Thin shell. No transverse shear deformation
Mass elements	1033	
Rigid body elements	507	

Table 2 Material properties (linear elastic constitutive model)

Building	Young's modulus (GPa)	Poisson's ratio
Reactor containment building (RCB)	30.45	0.17
RCB internal structures	30.45	0.17
Auxiliary complex building (ACB)	27.77	0.1694
Rigid beams at the bottom of stick models	2777	0

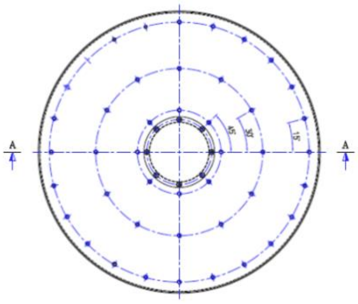

(a) Plane view of the bearing

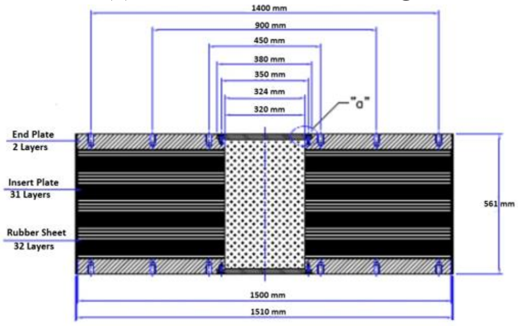

(b) Vertical cut view along A-A section

Fig. 2 Isolator unit used by PEER (UNISON e-Tech Co.)

Table 3 Gravity loads

Names	Fixed Model (kip)	ANT 486 (kip)	ANT 005 (kip)
Weight of NI-Buildings	831499	831499	831499
Weight of NI-Mat	231778.25	231777.86	231645.48
Weight of Pedestals	0	33874	0
Total Weight of Model	1063278	1097151	1063277

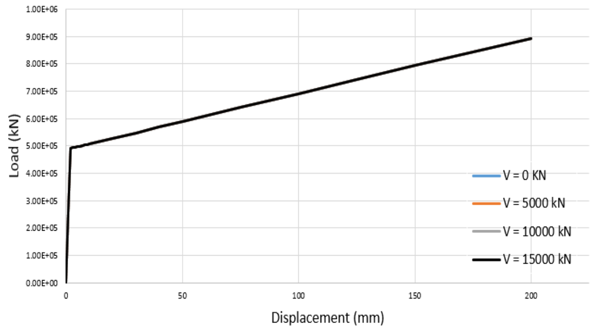

(a) Load-displacement behavior of the isolator

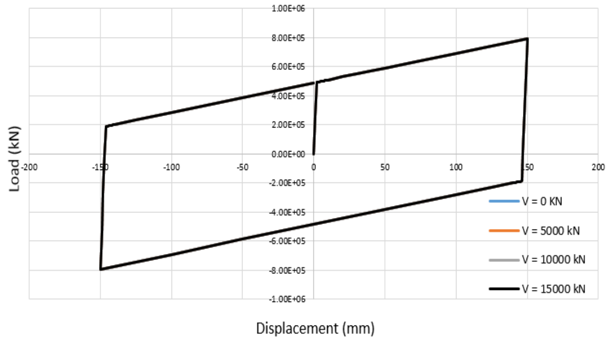

(b) Hysteretic behavior of the isolator

Fig. 3 Isolator model and its behavior

NI includes reactor systems, internal structures and containment structures of reactor containment building (RCB), auxiliary complex building (ACB), and an upper basemat supporting the RCB and ACB. For the purposes of benchmark, the upper basemat is considered to be rigid. Table 2 provides the material properties of the linear elastic constitutive models considered for the superstructure.

An experimental model of LRB unit used in this ANT structure produced by Unison e-Tech were used by Pacific Earthquake Engineering Research center (PEER) in collaboration with the Korean Electric power company KEPCO E&C as an effort to practically implement the base-isolation technology for the NPP industry. The bearing is 1500 mm in diameter in total and a 320-mm-diameter for lead core; as shown in Fig. 2. Thirty-two, 7-mm-thick rubber layers resulted in a total rubber thickness of 224 mm. These layers were sandwiched between 31, 7-mm-thick steel plates and 60-mm-thick end plates, resulting in a total bearing height of 527 mm. The zero-displacement force intercept, Q_d, was specified as 670 kN. Initial stiffness, K_1, and second slope stiffness, K_2, were calculated and verified by Unison e-Tech to be 351 kN/mm and 3.4 kN/mm (*et al*. 2015).

The numerical model of the ANT does not consider a moat wall, backfill, or the soil foundation. The single unit of the total isolation system is termed as a bearing. The lower basemat and the bearing pedestals are modelled as being fixed base. The stick model is therefore connected to different sets of isolators, which in turn gives two different computational models: 1) 486-bearing model (ANT 486), 2) Five-bearing equivalent model (ANT 005).

The properties considered for the selective structural models are provided under the specific section of structural models. The numerical model of the isolator is analyzed under both Quasi-static and 500mm/sec dynamic loading condition. Fig. 3(a) signifies the load-displacement behavior and Fig. 3(b) hysteretic behavior of the isolator for 500mm/sec condition. In this study, the coupling effect between the horizontal and vertical loading is not considered. It can be seen from Fig. 3 that isolators under different vertical loading gives the same load displacement behavior as well as hysteretic behavior.

2.2 486-bearing model (ANT 486)

Fig. 4(a) shows the arrangement of 486 bearings and 4(b) shows the structural model in the OpenSees module. In

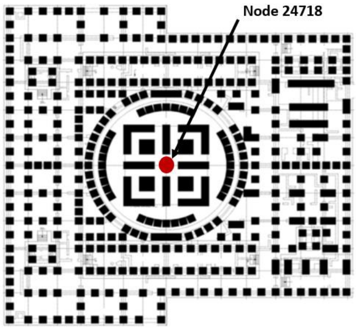

(a) Arrangement of 486 bearings

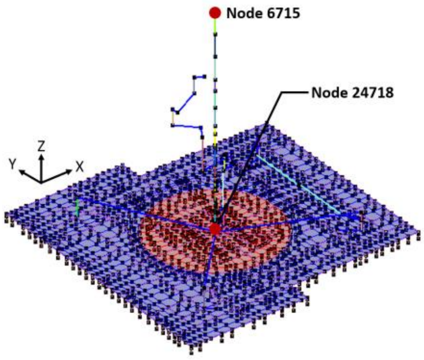

(b) 486- bearing model in OpenSees

Fig. 4 486-bearing structural model (ANT 486)

Table 4 Bearing properties of ANT 486

No.	Direction	Linear		Nonlinear		
		Stiffness	Damping	Stiffness	Yield Strength	Post Yield Strength Ratio
	X	883,867.60	1,088.46	-	-	-
1	Y	614.91	135.24	36,844.36	226.98	7.82E-03
	Z	614.91	135.24	36,844.36	226.98	7.82E-03

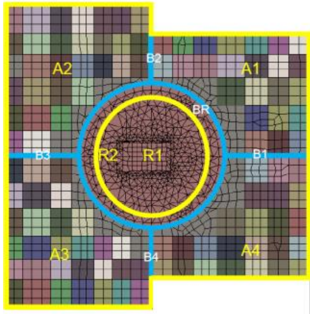

(a) Area division for 5-bearing equivalent model

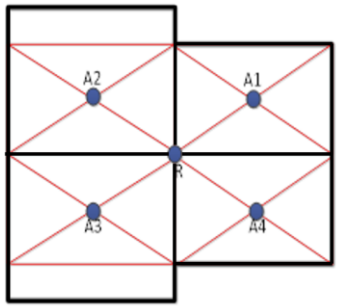

(b) Location of five-bearing equivalent model

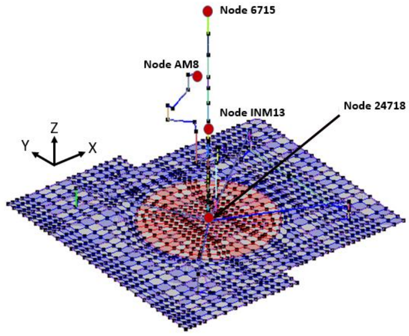

(c) 5-bearing equivalent model in OpenSees

Fig. 5 Five-bearing equivalent model (ANT 005)

this structural model, the lower end of each bearing is fixed and the upper end is connected to the upper basemat which is modeled by 2,570 plate elements.

The bearings of ANT 486 model have been modeled explicitly as beam elements connecting the foundation to the basemat in the OpenSees. Table 4 provides the linear and nonlinear structural properties of bearing that has been considered for ANT 486. In this model, all bearings are assumed to have same properties as assumed in table 4 uniformly.

2.3 5-bearing equivalent model (ANT 005)

The 5-bearing equivalent model (ANT 005) has been named after the 5-bearings, adopted for this structure that represent the equivalent properties of 486 bearings. Fig. 5(a) shows the area division of the total basemat area to allocate the centroid for isolator installation. After that, the location found from the area division calculation is showed in Fig. 5(b). Finally, Fig. 5(c) represent the 5-bearing equivalent model (ANT 005) in the OpenSees. The vertical, horizontal, and torsional stiffness of the equivalent bearing are calculated by the following equations

$$k_v = num_{Iso} \times k_{v,Iso} \tag{1}$$

$$k_{F_y} = num_{Iso} \times k_{h,Iso} \tag{2}$$

$$k_{F_z} = num_{Iso} \times k_{h,Iso} \tag{3}$$

$$k_T = \sum_{i=1}^{num_{Iso}} k_{h,Iso} \times R_i^2 \tag{4}$$

where k_v is the equivalent vertical stiffness; num_{Iso} is the number of bearing; $k_{v,Iso}$ is the vertical stiffness of each bearing; k_{F_y} and k_{F_z} are the equivalent horizontal stiffness; k_T is the equivalent torsional stiffness; $k_{h,Iso}$ is the equivalent horizontal stiffness; and R is the distance between the center of each bearing and the centroid of all bearings. The rigid links are connected between the 5 equivalent bearings and the upper basemat as shown in red lines in Fig. 5(b).

Table 5 Properties of base-isolator of ANT 005

No.	Direction	Linear		Nonlinear		
		Stiffness	Damping	Stiffness	Yield Strength	Post Yield Strength Ratio
1	X	89,270,628	19,634,283			
	Y	62,106	13,659.64	3,518,272	22,062.46	7.82E-03
	Z	62,106	13,659.64	3,518,272	22,062.46	7.82E-03
	XX	2.78E+08	6.12E+07	-	-	-
	YY	1.69E+11	3.72E+10	-	-	-
	ZZ	2.31E+11	5.08E+10	-	-	-
2	X	75,128,746	16,523,901	-	-	-
	Y	52,267	11,495.74	3,581,272	22,062.46	7.82E-03
	Z	52,267	11,495.74	3,581,272	22,062.46	7.82E-03
	XX	2.53E+08	5.57E+07	-	-	-
	YY	1.92E+11	4.22E+10	-	-	-
	ZZ	1.72E+11	3.79E+10	-	-	-
3	X	68,057,805	14,968,711	-	-	-
	Y	47,348	10,413.79	3,581,272	22,062.46	7.82E-03
	Z	47,348	10,413.79	3,581,272	22,062.46	7.82E-03
	XX	1.94E+08	4.26E+07	-	-	-
	YY	1.22E+11	2.69E+07	-	-	-
	ZZ	1.56E+11	3.44E+10	-	-	-
4	X	74,244,878	16,392,502	-	-	-
	Y	51,652	11,360.50	3,581,272	22,062.46	7.82E-03
	Z	51,652	11,360.50	3,581,272	22,062.46	7.82E-03
	XX	2.28E+08	5.00E+07	-	-	-
	YY	1.21E+11	2.66E+10	-	-	-
	ZZ	2.06E+11	4.53E+10	-	-	-
5	X	122,900,000	27,021,439	-	-	-
	Y	85,472	18,798.92	3,581,272	22,062.46	7.82E-03
	Z	85,472	18,798.92	3,581,272	22,062.46	1.01E+00
	XX	3.62E+08	7.95E+07	-	-	-
	YY	2.65E+11	5.82E+10	-	-	-
	ZZ	2.55E+11	5.62E+10	-	-	-

Table 5 gives the linear and nonlinear isolator properties adopted for 5-bearing equivalent model (ANT 005). Based on the area and equivalence calculation 5 different isolators was adopted for this structural model. After the isolator modeling, the structural model of the 5-bearing equivalent model has been verified by OpenSees through modal analysis and comparing their modal frequencies and mode shapes with 486 bearing model BI-NPP. The modal effective mass of both structural model is illustrated at table 6 where the modal frequencies are discussed in the modal analysis section. The Rayleigh approach for the modelling of damping is used in the analyses, with no mass proportional damping (α=0) and stiffness proportional damping (β) computed so that 0.6% damping is obtained at 0.5 Hz. No stiffness proportional damping was used for the isolators (β=0 in the isolators).

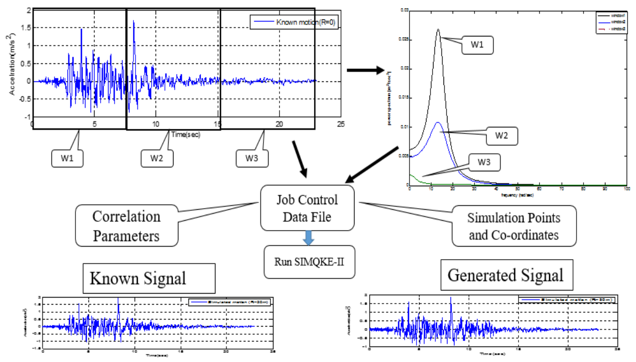

Fig. 6 SIMQKE-II procedure steps to simulate spatially correlated earthquake ground motions

3. Incoherent earthquake motions generation

3.1 SIMQKEII GM generation scheme

In this study, the conditional simulation of a reference earthquake motion Kocaeli has been done by the computer program SIMQKE-II. Fig. 6 illustrates the SIMQKE-II procedure for simulating spatially correlated earthquake ground motions at required distances. Also, Fig. 6 demonstrates the basic input parameters for SIMQKE-II as: 1) a known recorded acceleration time history, 2) spectral density function calculated from the known time history for several windows (size of the windows must be $2n^2$ where n

Table 6 Modal effective mass

Mode	$\mathbf{M_x}$ (kg)		$\mathbf{M_y}$ (kg)		$\mathbf{M_z}$ (kg)	
	ANT486	ANT05 eq.	ANT486	ANT05 eq.	ANT486	ANT05 eq.
1	0	4828531.1	488255466	478024579	0	0
2	488255466	478024579	0	4828531.1	0	0
3	0	0	0	0	0	0
4	0	0	0	0	0	0
5	0	0	0	0	0	0
6	0	0	0	0	0	4823553.12
7	0	0	0	0	0	0
8	0	0	0	0	0	4823553.12
9	0	0	0	0	0	0
10	0	0	0	0	0	202589231
11	0	0	0	0	278724357	125412381
12	0	0	0	0	4977220.65	9647106.24
13	0	0	0	0	49772206.5	4823553.12
14	0	0	0	0	0	0
15	0	0	0	0	24886103.3	14470659.4
16	0	0	0	0	0	0
17	0	0	0	0	0	0
18	0	0	0	0	4977220.65	4823553.12
19	0	0	0	0	4977220.65	0
20	0	0	0	0	14931662	19294212.5

is positive integer numbers), 3) location of simulation point where the simulated motion is required, 4) the frequency-dependent spatial correlation function proposed by Vanmarcke *et al*. (1999).

The isotropic frequency dependent spatial correlation function proposed by Vanmarcke (1999) is expressed as follow

$$\rho_{\omega k}(r_{ij}) = \exp\left\{\frac{-\omega_k|r_{ij}|}{2\pi cs}\right\} \tag{5}$$

where, r_{ij} is the relative position vector between the recorded and simulated ground motions, c is the shear wave velocity of the soil medium, and s is the distance-scale parameter. Through changing the distances between the recorded and simulated ground motions while fixing the distance-scale parameter value, the degree of correlation can be controlled. As per ASCE 7-10 (2010), in this study, the incoherent motion is generated for hard rock soil as well as soft rock soil. Therefore, the shear wave velocity is assumed to be 2500 m/sec for hard rock, and 300 m/sec. for soft soil. The algorithm used in SIMQKE-II is described herein briefly. If the acceleration ground motion at any location $x_i$is a homogenous mean-square continuous real-time process, it can be expressed as a sum of an independent sinusoidal process K at discrete frequencies each separated by $\Delta\omega$ as

$$Z_i(t) = \sum_{k=0}^{K-1}[A_{ik}\cos(\omega_t t) + B_{ik}\sin(\omega_t t)] \tag{6}$$

The random coefficients A_{ik} and B_{ik} are related to $Z_i(t)$ through discreet Direct Fourier Transform (DFT) in case of discrete time and to generate $Z_i(t)$ at times $t_j = j\Delta t, j = 0,1,\ldots,K-1$

$$A_{ik=} \frac{1}{K}\sum_{j=0}^{K-1} Z_i(t_j)cos\left(\frac{2\pi k_j}{K}\right),$$
$$B_{ik=} \frac{1}{K}\sum_{j=0}^{K-1} Z_i(t_j)sin\left(\frac{2\pi k_j}{K}\right) \tag{7}$$

The following algorithm is implemented in SIMQKE-II to generate conditionally spatially varying ground motions (Vanmarcke *et al*. 1999):

(1) For each frequency $\omega_k, k = \frac{K}{2},\ldots,K-1$: Assembling the frequency specific covariance matrix $C_k$as

$$C_{ij}(\omega_k)\begin{cases} 0.5\rho_{\omega k}(r_{ij})G(\omega_k)\Delta\omega, \quad for\ k=0 \\ 0.25\{\rho_{\omega k}(r_{ij})G(\omega_k) + \rho_{\omega K-k}(r_{ij})G(\omega_{K-k})\}, \\ for\ k = 1,..,\frac{K}{2}-1 \\ 1.0\ \rho_{\omega k}(r_{ij})G(\omega_k)\Delta\omega, \\ for\ k = K/2 \end{cases} \tag{8}$$

and

$$C_k = \begin{bmatrix} C_{\alpha\alpha} & C_{\alpha\beta} \\ C_{\alpha\beta}^T & C_{\beta\beta} \end{bmatrix} \tag{9}$$

where $r_{ij} = x_i - x_j$ is the relative position vector, where x_i and x_j are the two spatial points. $G(\omega_k)$ is the one-sided spectral density function, and $\rho_{\omega k}(r_{ij})$ is the frequency-dependent spatial correlation function. In addition, considering that the simulation of earthquake ground motion at a set of m target (unknown) points given that some motions have been recorded at the set of $n = N - m$ recording (known) points, where N is the total number spatial location points under consideration. Moreover, $C_{\alpha\alpha}$ is the covariance matrix between known (recording) points, $C_{\beta\beta}$ is the covariance matrix between unknown (target) points, and $C_{\alpha\beta}$ is the covariance matrix between known and unknown points, at all frequencies ω_k. The admissible spatial correlation function and spectral density function, $\rho_{\omega k}(r_{ij})$ and $G(\omega_k)$ and the matrix C_k is positive and can be expressed as the product of lower triangular matrix L_x and its transpose by means of Cholesky decomposition.

$$C_k = L_k L_k^T \tag{10}$$

Simulating the sets of unconditioned Fourier confections A_s and B_s using

$$A_s = L_k U_{k,}\ B_s = L_k V_k \tag{11}$$

Computing the Best Linear Unbiased Estimators (BLUE) estimators A_α^* and B_α^* using the known coefficients A_α and $\beta_\alpha$using

$$A_\alpha^* = C_{\alpha\beta}^T C_{\alpha\alpha}^{-1} A_\alpha, \qquad B_\beta^* = C_{\alpha\beta}^T C_{\alpha\alpha}^{-1} B_\alpha \tag{12}$$

Computing the BLUE estimators $A_{s\alpha}^*$ and $B_{s\alpha}^*$ using the simulated coefficients $A_{s\alpha}$ and $B_{s\alpha}$at the known points according using

$$A_{s\beta}^* = C_{\alpha\beta}^T C_{\alpha\alpha}^{-1} A_{s\alpha}, \qquad B_{s\beta}^* = C_{\alpha\beta}^T C_{\alpha\alpha}^{-1} B_{s\alpha} \tag{13}$$

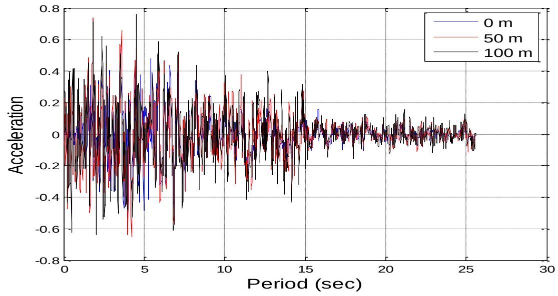

(a) Soft rock site

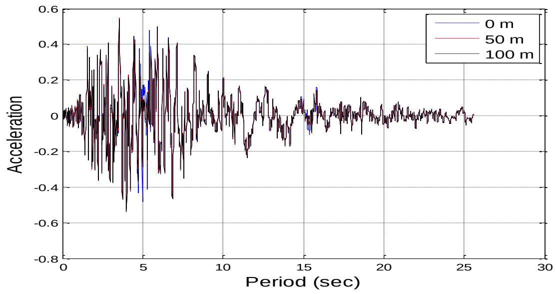

(b) Hard rock site

Fig. 7 Simulated acceleration time histories at different locations

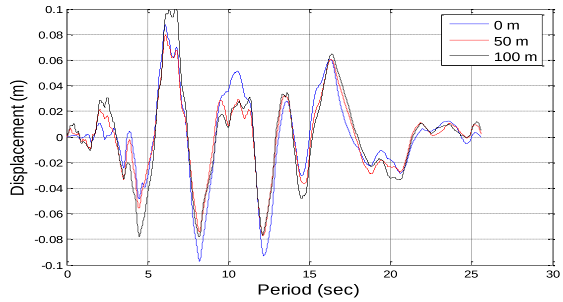

(a) Soft rock soil

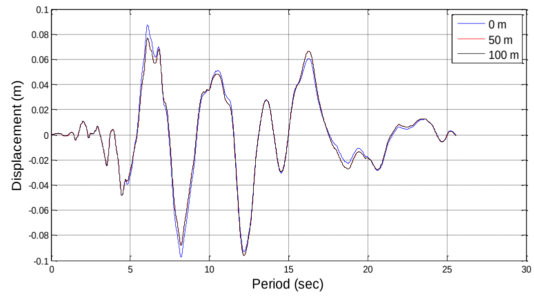

(b) Hard rock soil

Fig. 8 Simulated displacement time histories at different locations

(2) Generating the conditional Fourier coefficients at the unknown points A_c and B_c as follows

$$A_c = A^*_\beta + A_{s\beta} - A^*_{s\beta},\ B_c = B^*_\beta + B_{s\beta} - B^*_{s\beta} \tag{14}$$

(3) Generating the remaining Fourier coefficients at frequencies $\omega_k, k = \frac{K}{2}, \ldots, K-1$ using the symmetry conditions

$$A_{ik} = A_{i,K-k}, \qquad B_{ik} = B_{i,K-k}, \qquad for\ k = 1,2,\ldots,K/2 \tag{15}$$

Applying an inverse FFT to construct the field of time histories at the unknown target points.

3.2 Conditionally simulated ground motions

In conditional simulations, the generated ground motions are statistically compatible with (conditioned by) the recorded ground motions at nearby points. The generated ground motions are more closely correlated to the reference ground motions when they become increasingly dependent and similar to the reference ground motions.

Fig. 7 shows the known acceleration time series at 0 m and generated incoherent time series at 50 m and 100 m of selected motion Kocaeli. Fig. 7(a) represent the generated incoherent motions for soft soil (soil shear velocity 300 m/s) whereas Fig. 7(b) presents the generated incoherent motions for hard rock soil (soil shear velocity 2500 m/s). These generated accelerations are simulated from a real recorded motion and therefore called spatially correlated conditionally ground motions.

After generating the correlated conditionally simulated ground motions using SIMQKE-II at the target locations for rock site conditions with 50 m spacing, a suggested processing scheme for simulation and conditional simulation by Liao and Zerva (2006) is used to extract the displacement time histories from simulated artificial acceleration histories. In the suggested scheme, the high-pass filter is applied to the acceleration time histories, followed by double integration of the acceleration to extract the displacement time histories. The most commonly used filter, by the US Geological Survey (USGS) and the Pacific Earthquake Engineering Research Center (PEER) is the Butterworth filter (Zerva 2009). Which implies that at least 98% of the low frequency components with a period longer than the ground motions time history duration are filtered out. Fig. 8(a) represents the displacement motions for soft soil and Fig. 8(b) represents the same for hard rock soil. It can be noticed that motions for hard rock shows better similarity than soft rock soil. These integrated displacement time histories are used as multi-support excitation at the BI-NPP foundation mat nodes at the different target distances along the longitudinal direction (*X*-direction).

The simulated ground motions at 50 m and 100 m show relatively high correlation with the known ground motions as expected, due to assuming the distance-scale parameter value to be 5, which refers to a high correlation between the known and simulated ground motions. Fig. 9(a) illustrates the acceleration response spectra of the known and simulated ground motions at 5% damping for soft soil incoherent motion and Fig. 9(b) shows the same for hard rock soil. The similarity between simulated motions for hard rock is better than soft rock soil that can be noticed from Fig. 9 comparatively.

3.3 Lagged coherency

The lagged coherency, $\gamma_{ij}(i\omega)$, is a measure of

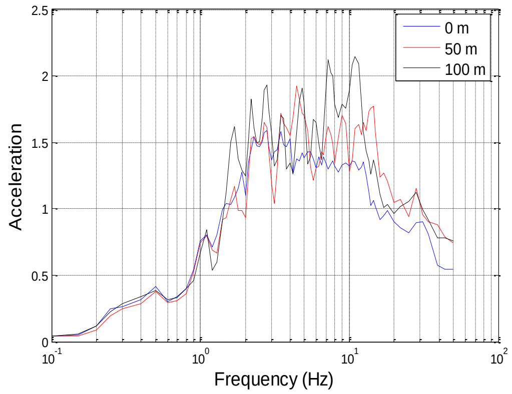

(a) Soft rock site

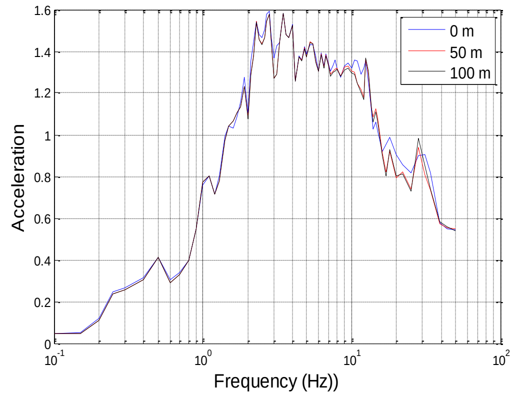

(b) Hard rock site

Fig. 9 Acceleration response spectra of simulated ground motions (5% damping ratio)

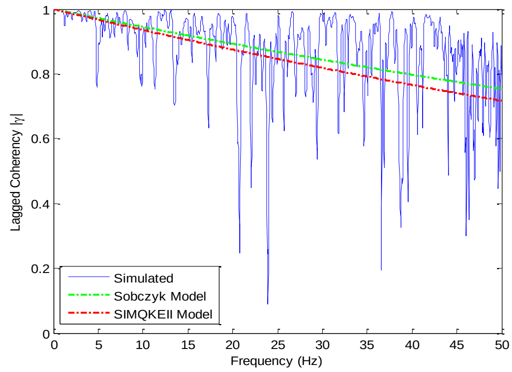

(a) Coherency loss at 50 m

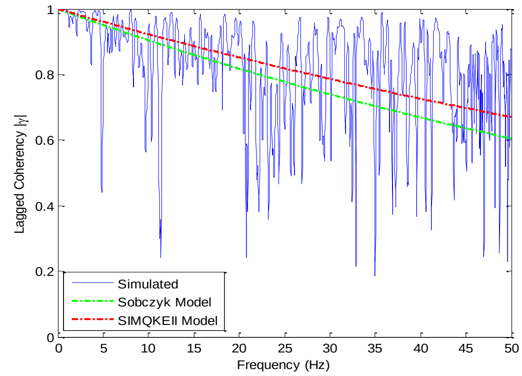

(b) Coherency loss at 100 m

Fig. 10 Coherency loss between known and generated motions

"similarity" in the seismic motions, and indicates the degree to which the data recorded at the two stations are related by means of a linear transfer function. SIMQKE model and the Sobczyk model (Sobczyk 1991, Bi and Hao 2012) are selected to investigate the coherency loss between the reference and simulated ground motions. The Sobczyk model is selected to describe the coherency loss between the ground motions at points i and j where $i \neq j$

$$\gamma_{ij}(i\omega) = \left|\gamma_{ij}(i\omega)\right| \exp\left(-\frac{i\omega_{ij} cos\alpha}{V_{app}}\right) \\ = \exp\left(-\frac{\beta\omega d_{ij}^2}{V_{app}}\right).\exp\left(-\frac{i\omega_{ij} cos\alpha}{V_{app}}\right) \tag{16}$$

where β is a coefficient which reflects the level of coherency loss, $\beta = 0.0005$ is used in the present paper, which represents highly correlated motions; d is the distance between the points i and j, and d_{ij}=100 m and 50 m is assumed; α is the incident angle of the incoming wave to the site, and is assumed to be 0°; (as we are not considering any influence of incident angle and the ground motion excitations are applied along longitudinal direction only); V_{app} is the apparent wave velocity in the bedrock, which is 2500 m/s which represent hard rock soil and 300 m/s for soft rock soil.

Fig. 10 illustrates the coherency loss between known and generated motion, and the prescribed models using equation 16. Fig. 10(a) shows the coherency loss at 50 m whereas Fig. 10(b) shows the same at 100 m. Good matching between the models and the simulated coherency loss functions is observed. On the other hand, it can be noticed that the loss is significant at 100 m compared to the coherency loss at 50.

4. Result

To examine the effect of incoherent ground motion, the reference uniform motion Kocaeli, and stochastically simulated incoherent ground motions are applied along longitudinal direction of BI-NPP as uniform and multi-support excitation respectively. Two types of model i.e., ANT 486 bearing model and ANT 005 equivalent isolators are analyzed and result of seismic response are investigated, presented in the following sections.

4.1 Modal analysis

The Eigen analysis is done for all both BI-NPP structural model to get their natural frequency for three major modes governed by the isolators. The obtained natural frequency is 0.477 Hz for ANT486 and ANT005 equivalent models for first mode. The target natural frequency is 0.5 Hz and the obtained frequency is almost close to target frequency.

Also, the modal participation ratio is same for all cases and its about 100%. Fig. 11 and Fig. 12 shows the 3D mode

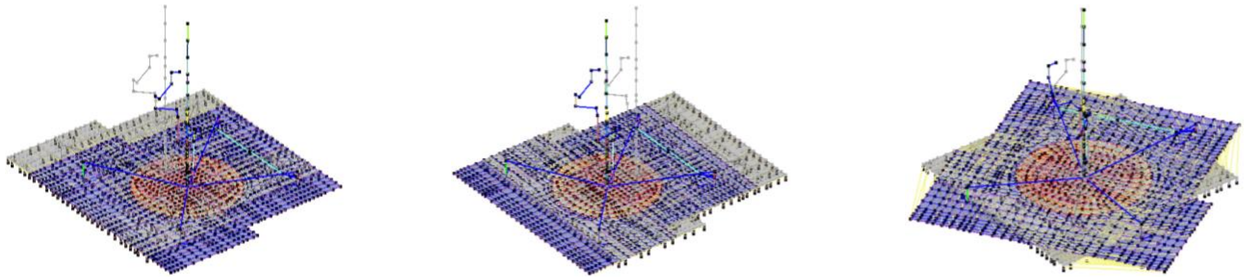

(a) 1st mode shape (0.477 Hz) (b) 2nd mode shape (0.477 Hz) (c) 3rd mode shape (0.710 Hz)

Fig. 11 Modal shapes of ANT 486 bearing model

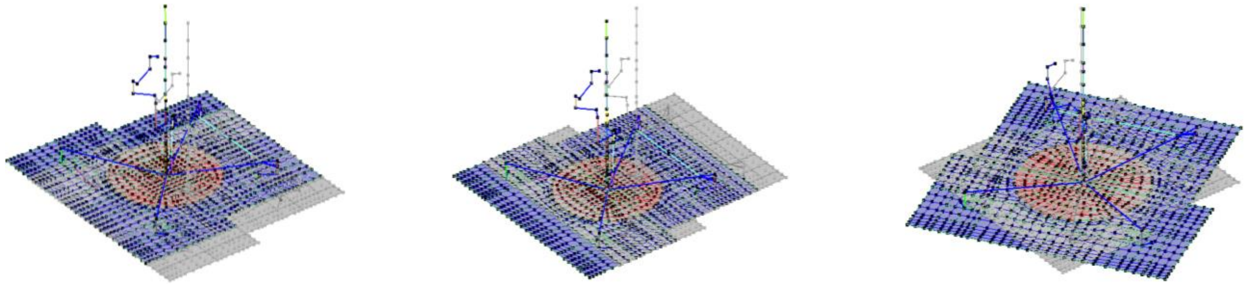

(a) 1st mode shape (0.477 Hz) (b) 2nd mode shape (0.477 Hz) (c) 3rd mode shape (0.711 Hz)

Fig. 12 Modal shapes of ANT 005 bearing equivalent model

Table 7 Modal frequencies of structures

Mode No.	ANT 486 model (Hz)	ANT 005 Model (Hz)
1st mode	0.477	0.477
2nd mode	0.477	0.477
3rd mode	0.710	0.711

shapes of ANT486 and ANT005 models respectively. Modal frequencies of each mode are summarized in the same figures. Both models were verified by the modal analysis where modal frequency were checked found to be at the same value. Table 7 summarizes the modal frequencies for both structure for first three modes being governed by the behavior of isolators.

4.2 Earthquake analysis

Seismic Input Motion following US NRC RG 1.60/ DBE (PGA=0.50 g) time history analysis conducted using Newmark-beta method. Fig. 13 presents the ratio of maximum horizontal acceleration responses between uniform motion excitation to incoherent motion excitation for Kocaeli earthquake and both structural model. When the magnitude of the ratio is greater than 1.0, it signifies the maximum acceleration response from uniform motion is greater than incoherent motion and vice versa. The ratio has been investigated for both top node (node 6715) and bottom node (node 24718) of both structural model and it is noticeable that except for lower frequencies, the ratio is always greater than 1.0. Therefore, Fig. 13(a) and Fig. 13(b) clearly signifies the reduction of maximum acceleration responses due to incoherent motion for soft rock soil as well as hard rock soil respectively.

Fig. 14(a) and Fig. 14(b) gives the displacement response of the isolator (node 24718) for hard rock soil

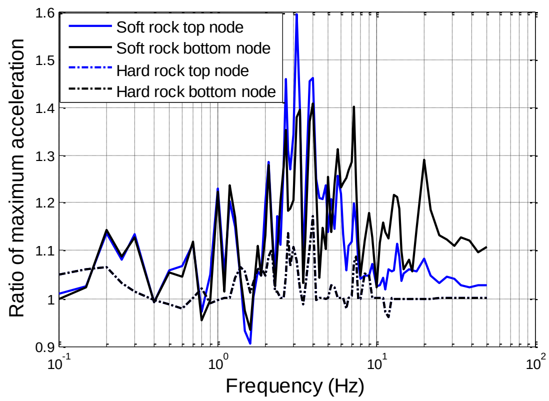

(a) ANT 486

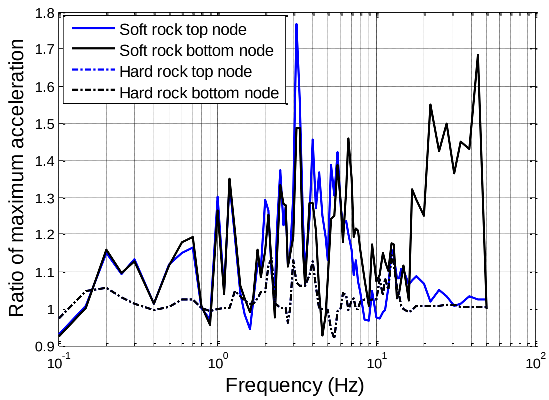

(b) ANT 005

Fig. 13 Ratio of maximum acceleration response

incoherent motion for ANT 486 bearing model and ANT 005 model respectively. Decrease in the maximum response for incoherent motion is visible for both structural model. It has been noticed that incoherent motions generated for soft

Table 8 Percentage reduction in the maximum displacement

Node	ANT 486		ANT 005	
	Soft rock soil (%)	Hard rock soil (%)	Soft rock soil (%)	Hard rock soil (%)
Node 6715	10.72	8.13	11.88	8.40
Node 24718	7.44	8.67	11.62	8.80

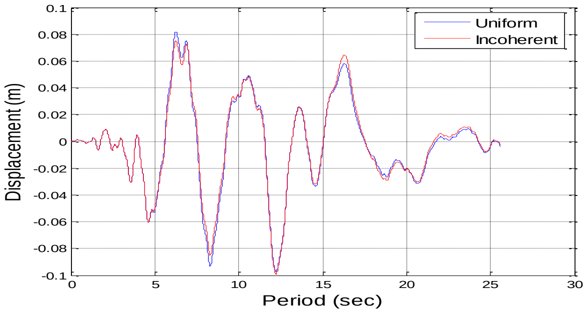

(a) ANT 486

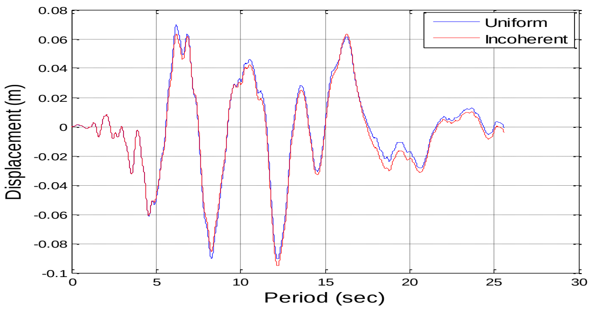

(b) ANT 005

Fig. 14 Lateral displacement response of the isolator for hard rock soil

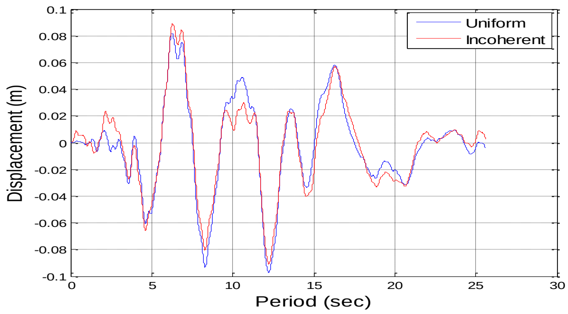

(a) ANT 486 Bearing model

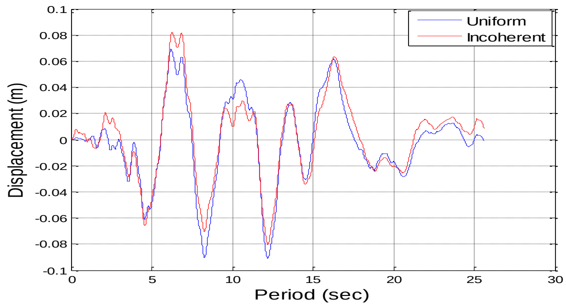

(b) ANT equivalent 5 bearing model

Fig. 15 Lateral displacement response of the isolator for soft rock soil

soil shows significant high frequency content than hard rock soil. Therefore, the effect of incoherent motion is convincingly noticeable for soft soil case in Fig. 14(a) and Fig. 14(b). In addition, Fig. 15(a) and Fig. 15(b) gives the comparison of displacement response between uniform motion to incoherent motion for soft rock soil respectively. Table 8 describes the percentage decrease in the maximum displacement for both structural model and both incoherent motion types. The noticeable comparison here is the significant decrease in displacement response, soft rock soil shows higher reduction and ANT 5 equivalent bearing model shows a slight higher reduction in the displacement response which means higher the number of isolators lowers the percentage reduction.

Fig. 16(a) and Fig. 16(b) demonstrates the acceleration response spectra of node 24718 under Kocaeli earthquake of ANT486 model for soft rock soil and hard rock soil respectively. On the other hand, Fig. 17(a) and Fig. 17(b) presents the same for ANT005 strucutral model for soft rock soil and hard rock soil respectively. Clearly, it can be noticed that for both structural model, incohernce has reduced the acceleration, particularly in the high frequencies, the differnce are noticeable. Seismic analyses incorporating ground motion incoherence demonstrate a significant reduction in high-frequency seismic response as measured by isolator acceleration response spectra. The

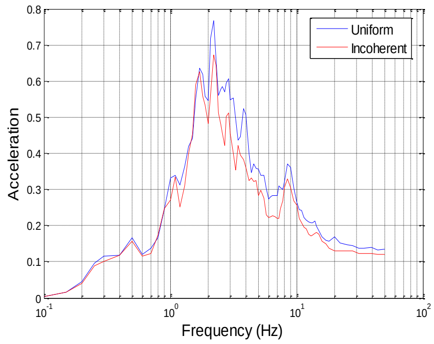

(a) Response spectra for soft soil

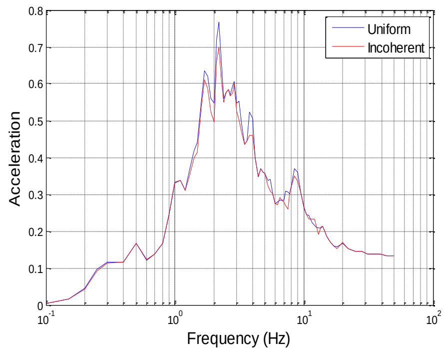

(b) Response spectra for hard rock

Fig. 16 Acceleration response spectra of isolator node 24718 adopted at ANT486 model (5% damping)

effect of seismic incoherence is primarily a high-frequency phenomenon. It has been observed that for soft soil the generated acceleration ground motions contains more high-frequency than hard rock soil. Therefore, the response reduction is much visible for soft rock soil compared to

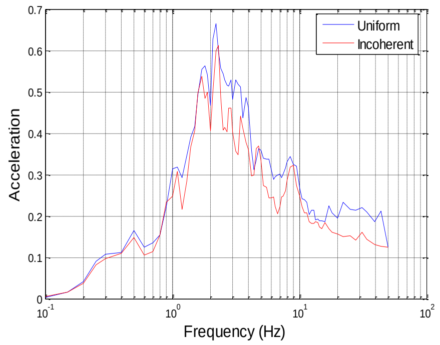

(a) Response spectra for soft soil

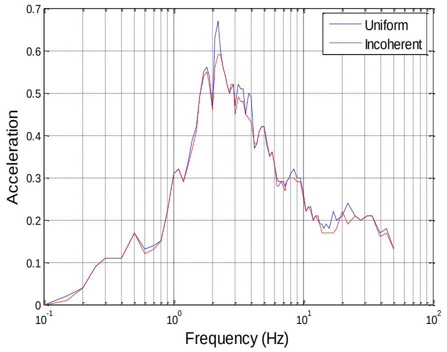

(b) Response spectra for hard rock

Fig. 17 Acceleration response spectra of isolator node 24718 adopted at ANT005 model (5% damping)

response reduction seen for hard rock soil. Furthermore, this phenomenon has been observed for both structural model simultaneously.

It has been investigated that for soft rock soil ANT005 model gives 18.45% reduction of acceleration response in the bottom and 8% reduction in the top node. On the other hand, the reduction is comparatively small for hard rock soil which is 6% in the bottom and 11% in the top node. The statistical comparison between the acceleration response reduction for base-isolator with high stiffness also shows a significant reduction in the responses which is 15.24% for top node and 4.8% for bottom node for soft rock soil. For hard rock soil the reduction is smaller which is 1.3% for top node and 0.5% for bottom node.

5. Conclusions

The investigation of incoherent motion effect on the seismic response is conducted on two structural models: 486 Isolator (ANT 486) and 5 equivalent isolator (ANT 005) models. Both models are investigated under two different types of input excitations: uniform motion and incoherent motion. Based on the investigation conducted in this study, the following conclusion can be summarized for the selected input motion of Kocaeli, and BI-NPP structure.

• The incoherent motion generated from the selected motion shows significant reduction in the seismic responses like lateral displacements, maximum accelerations and ratio of maximum acceleration. The reduction is significant at higher frequencies for both ANT models.

• Floor acceleration responses due to uniform motion were noticeably higher compared to incoherent motions for wide range of frequency for this particular reference earthquake. The difference is apparent at higher frequencies, particularly where the maximum response occurs.

• The percentage reduction of the seismic response especially maximum displacement and maximum acceleration for 5 bearing equivalent model is minimally higher compared to ANT 486 bearing model.

•The effect of the incoherent motion generated from the selected motion considering soft soil and hard rock soil is investigated, and the effect is much significant in the soft soil sites.

In the end, while this research demonstrates the necessity of incorporation of incoherent motion effect in the seismic design of isolated ANT NPP structure using only one reference motion, additional studies must be carried out in future with a variety of motion and isolation systems to implement this concept.

Acknowledgements

This work was supported by the Korea Institute of Energy Technology Evaluation and Planning (KETEP) and the Ministry of Trade, Industry & Energy (MOTIE) of the Republic of Korea (No. 20171510101960).

References

Abrahamson, N.A. (1993), “Spatial variation of multiple supports inputs”, *Proceedings of the 1st US Seminar on Seismic Evaluation and Retrofit of Steel Bridges*, A Caltrans and Univ. of California at Berkeley Seminar, San Francisco CA.

Abrahamson, N. (2005), “Spatial coherency for soil-structure interaction”, Electric Power Research Institute, Technical Update Report 1012968, Palo Alto, CA, December.

Abrahamson, N. (2007), “Effects of seismic motion incoherency effects”, EPRI Palo Alto, CA, TR-1015111

Abrahamson, N.A., Schneider, J.F. and Stepp, J.C. (1991), “Empirical spatial coherency functions for applications to soil-structure interaction analyses”, *Earthq. Spectra*, **7**, 1-27.

Adanur, S., Altunisik, A.C., Soyluk, K., Dumanoðlu, A.A. and Bayraktar, A. (2016), “Contribution of local site-effect on the seismic response of suspension bridges to spatially varying ground motions”, *Earthq. Struct.*, **10**(5), 1233-1251.

Ahmed, K. and Kim, D. (2017), “A windowed adjustment function based NRC compliant ground motions for fragility analysis of base-isolated nuclear power plant”, *KSCE J. Civil Eng.*, 1-11.

Ali, A., Hayah, N.A., Kim, D. and Cho, S.G. (2014), “Probabilistic seismic assessment of base-isolated NPPs subjected to strong ground motions of Tohoku earthquake.”, *Nucl. Eng. Technol.*, **46**(5), 699-706..

American Society of Civil Engineers (ASCE) (2010), Minimum Design Load for Buildings and Other Structures, ASCE/SEI 7-10, ASCE, Reston, VA.

American Society of Civil Engineers (ASCE), Seismic Analysis of Safety-Related Nuclear Structures, ASCE/SEI 4-**, Reston, VA.

Chakraborty, A. and Basu, B. (2008), “Nonstationary response analysis of long span bridges under spatially varying differential support motions using continuous wavelet transform", *J. Eng. Mech*., ASCE, **134**(2), 155-162.

Der Kiureghian, A. and Neuenhofer, A. (1992), "Response spectrum method for multiple support seismic excitation", *Earthq. Eng. Struct. Dyn*., **21**, 713-740.

Der Kiureghian, A., Keshishian, P. and Hakobian, A. (1997), "Multiple support response spectrum analysis of bridges including the site response effect and the MSRS code", Earthquake Engineering Research Center Report No. UCB/EERC-97/02, University of California, Berkeley, CA, USA.

EPRI (2005), Effect of Seismic Wave Incoherence on Foundation and Building Response, CA and the U.S. Department of Energy, 1012966.

EPRI (2006), Effect of Seismic Wave Incoherence on Foundation and Building Response, CA and the U.S. Department of Energy, Palo Alto, 1013504.

Ghaffarzadeh, H., Izadi, M.M. and Talebian, N. (2013), "Neural network-based generation of artificial spatially variable earthquakes ground motions", *Earthq. Struct.*, **4**(5), 509-525.

Hadidi, A., Azar, B.F. and Rafiee, A. (2016), "Reliability-based design of semi-rigidly connected base-isolated buildings subjected to stochastic near-fault excitations", *Earthq. Struct.*, **11**(4), 701-721.

Hao, H. and Duan, X.N. (1995), "Seismic response of asymmetric structures to multiple ground motions", *J. Struct. Eng.*, ASCE, **121**(11), 1557-1564.

Harichandran, R., Hawwari, A. and Sweidan, B. (1996), "Response of long-span bridges to spatially varying ground motion", *J. Struct. Eng*., **122**(5), 476-484.

Harichandran, R.S. (1987), "Stochastic analysis of rigid foundation filtering", *Earthq. Eng. Struct. Dyn.*, **15**, 889-899.

Harichandran, R.S. (1991), "Estimating the spatial variation of earthquake ground motion from dense array recordings", *Struct. Saf.*, **10**, 213-233.

Harichandran, R.S. and Vanmarcke, E.H. (1986), "Stochastic variation of earthquake ground motion in space and time", *J. Eng. Mech.*, ASCE, **112**(2), 154-174.

Hindy, A. and Novak, M. (1980), "Pipeline response to random ground motion", *J. Eng. Mech. Div*., ASCE, **106**, 339-360.

Huang, Y.N., Whittaker, A.S. and Luco, N. (2010), "Seismic performance assessment of base-isolated safety-related nuclear structures", *Earthq. Eng. Struct. Dyn.*, **39**, 1421-1442.

Huang, Y.N., Whittaker, A.S., Constantinou, M.C. and Malushte, S. (2007), "Seismic demands on secondary systems in base-isolated nuclear power plants", *Earthq. Eng. Struct. Dyn.*, **36**, 1741-1761.

Kim, S.H. and Feng, M.Q. (2003), "Fragility analysis of bridges under ground motion with spatial variation", *Int. J. Nonlin. Mech.*, **38**, 705-721.

Liao, S. and Zerva, A. (2006), "Physically-compliant, conditionally simulated spatially variable seismic ground motions for performance-based design", *Earthq. Eng. Struct. Dyn.*, **35**, 891-919.

Loh, C.H., Penzien, J. and Tsai, Y.B. (1982), "Engineering analysis of SMART-1 array accelerograms", *Earthq. Eng. Struct. Dyn.*, **10**, 575-591.

Luco, J.E. and Wong, H.L. (1986), "Response of a rigid foundation to a spatially random ground motion", *Earthq. Eng. Struct. Dyn*., **14**, 891-908.

Luco, J.E. and Wong, H.L. (1986), "Response of a rigid foundation to a spatially random ground motion", *Earthq. Eng. Struct. Dyn*., **14**, 891-908.

Malushte, S. and Whittaker, A.S. (2005), "Survey of past base isolation applications in nuclear power plants and challenges to industry/regulatory acceptance", *Proceedings of 18th International Conference on Structural Mechanics in Reactor Technology*, SMiRT 18, Beijing, China, August.

Mavronicola, E. and Komodromos, P. (2014), "On the response of base-isolated buildings using bilinear models for LRBs subjected to pulse-like ground motions: sharp vs. smooth behavior", *Earthq. Struct.*, **7**(6), 1223-1240

Monti, G., Nuti, C. and Pinto, P. (1996), "Nonlinear response of bridges under multi-support excitation", *J. Struct. Eng.*, **122**(10), 1147-1159.

Murase, M., Tsuji, M. and Takewaki, I. (2013), "Smart passive control of buildings with higher redundancy and robustness using base-isolation and inter-connection", *Earthq. Struct.*, **4**(6), 649-670.

Mwafy, A.M., Kwon, O.S., Elnashai, A. and Hashash, Y.M.A. (2011), "Wave passage and ground motion incoherency effects on seismic response of an extended bridge", *J. Bridge Eng.*, ASCE, **16**(3), 364-374.

Novak, M. and Hindy, A. (1979), "Seismic response of buried pipelines", *Proceedings of the 3rd Canadian Conference on Earthquake Engineering*, Montreal, Canada, January.

Saxena, V., Deodatis, G. and Shinozuka, M. (2000), "Effect of spatial variation of earthquake ground motion on the nonlinear dynamic response of highway bridges", *Proceedings of the 12th World Conference on Earthquake Engineering*, Auckland, New Zealand.

Sayed, M.A., Go, S., Cho, S.G. and Kim, D. (2015), "Seismic responses of base-isolated nuclear power plant structures considering spatially varying ground motions", *Struct. Eng. Mech.*, **54**(1), 169-188.

Schellenberg, A.H., Sarebanha, A., Schoettler, M.J., Mosqueda, G., Benzoni, G. and Mahin, S.A. (2015), "Hybrid simulation of seismic isolation systems applied to an APR-1400 nuclear power plant", PEER (Pacific Earthquake Engineering Research Center), Report No. 2015/05.

Schellenberg, A.H., Schoettler, M. and Mahin, S.A. (2015), "Review of ANT models and ground motions", PEER (Pacific Earthquake Engineering Research Center), Project Review Meeting, KEPCO E&C, South Korea November 16-17.

Shinozuka, M., Deodatis, G. and Saxena, V. (2000), "Effect of spatial variation of ground motion on bridge response," Technical Report MCEER-00-0013.

Sobczyk, K. (1991), *Stochastic Wave Propagation*, Kluwer Academic Publishers, Netherlands.

United States Nuclear Regulatory Commission (USNRC) (2012), Standard Review Plan for the Review of Safety Analysis Reports for Nuclear Power Plants, 3.7.2, Seismic System Analysis, NUREG-0800, USNRC, Washington, USA.

Vanmarcke, E., Heredia-Zavoni, E. and Fenton, G.A. (1993), "Conditional simulation of spatially correlated earthquake ground motion", *J. Eng. Mech.*, ASCE, **119**(11), 2333-2352.

Vanmarcke, E.H., Fenton, G.A. and Heredia-Zavoni, E. (1999), Conditioned Earthquake Ground Motion Simulator, SMIQKE-II User's Manual, Version 2.1.

Zerva, A. (1993), "Pipeline response to directionally and spatially correlated seismic ground motions", *J. Press. Ves. Tech*., ASME, **15**, 53-58.

Zerva, A. (2009), *Spatial Variation of Seismic Ground Motions: Modeling and Engineering Applications*, Taylor & Francis Group, CRC Press, Florida, USA.

Zerva, A. and Zervas, V. (2002), "Spatial variation of seismic ground motions: an overview", *Appl. Mech. Rev*., **55**(3), 271-297.

Zhao, C. and Chen, J. (2013), "Numerical simulation and investigation of the base isolated NPPC building under three-directional seismic loading", *J. Nucl. Eng. Des.*, **265**, 484-496.

CC